Received 3-8-17 RASch. Sent to g14 on 3-9-17

Beam-Target E asymmetries ~~from~~ for $\vec{\gamma}\vec{n} \to \pi^- p$ in the N* resonance region

D. Ho[3], P. Peng[16], C.D. Bass[1], P. Collins[4], A. D'Angelo[1,15], A. Deur[1], J.A. Fleming[13], C. Hanretty[1], T. Kageya[1], F.J. Klein[5],* E. Klempt[7], V. Laine[11], T.-S. H. Lee[2], M.M. Lowry[1], H. Lu[1]4, C. Nelapi[8], V.A. Nikonov[7,9], T. O'Connell[12], A.M. Sandorfi[1],* A.V. Sarantsev[7,9], R.A. Schumacher[3], I.I. Strakovsky[5], A. Švarc[10], N.K. Walford[4], X. Wei[1], C.S. Whisnant[6], R.L. Workman[5], I. Zonta[15], and ... a large cast from the CLAS collaboration

[1] *Thomas Jefferson National Accelerator Facility, Newport News, VA 23606, USA*
[2] *Argonne National Laboratory, Argonne, IL 60439, USA*
[3] *Carnegie Mellon University, Pittsburgh, PA 15213, USA*
[4] *Catholic University of America, Washington, DC 20064, USA*
[5] *George Washington University, Washington, DC 20052, USA*
[6] *James Madison University, Harrisonburg, VA 22807, USA*
[7] *Helmholtz-Institut für Strahlen- und Kernphysik, Universität Bonn, 53113 Bonn, Germany*
[8] *Old Dominion University, Norfolk, VA 23529, USA*
[9] *Petersburg Nuclear Physics Institute, Gatchina, 188300 Russia*
[10] *Rudjer Bošković Institute, Zagreb 10002, Croatia*
[11] *Université Blaise Pascal, Clermont-Ferrand, 63178 Aubière Cedex, France*
[12] *University of Connecticut, Storrs, CT 06269, USA*
[13] *University of Edinburgh, Edinburgh EH9 3FD, UK*
[14] *University of Iowa, Iowa City, IA 52242, USA*
[15] *Universita di Roma "Tor Vergata" and INFN Sezione di Roma2, 00133 Roma, Italy and*
[16] *University of Virginia, Charlottesville, VA 22903 USA*

(Dated: March 7, 2017)

We report the first beam-target double-polarization asymmetries in the $\gamma + n(p) \to \pi^- + p(p)$ reaction spanning the nucleon resonance region from W= 1500 to 2300 MeV. Circularly polarized photons and longitudinally-polarized deuterons in HD have been used with the CLAS detector at Jefferson Lab. The exclusive final state has been extracted using three very different analysis techniques, which ~~are in~~ show excellent agreement, and these have been used to deduce the E polarization observable for a neutron target. These results have been incorporated into new partial wave analyses, and have led to ~~improved~~ revised values for several γnN^* photo-couplings.

PACS numbers: 25.20.Lj, 13.88.+e, 13.60.Le, 14.20.Gk

A successful description of the excited levels of a composite system is a basic test of how well the underlying forces are understood. Although Quantum Chromodynamics is generally regarded as a mature theory describing interacting quarks within hadrons, the excited states of the nucleon pose many challenges. This partly arises because of the complexity of multiple effects that dress interactions and alter their manifestation, and partly because the states are broad and overlapping, making their production amplitudes difficult to disentangle without constraints from large numbers of measurements [1, 2]. Until relatively recently, excited baryon resonances were identified almost exclusively from πN scattering data, which yielded only a fraction of the number of levels expected [3, 4]. However recently, new candidate states have emerged from analyses of a large number of meson photoproduction experiments [5]. The associated γNN^* electromagnetic couplings in this expanded spectrum provided a measure of dynamical properties that serve as benchmarks for models of nucleon structure.

To isolate an excited nucleon state requires a decomposition of the reaction amplitude into multipoles of definite spin, parity and isospin. Single pseudo-scalar meson photoproduction is described by 4 complex amplitudes and requires data on a minimum of 8 (out of 16) different spin observables to avoid mathematical ambiguities, although in practice even larger numbers are needed to overcome the limitations imposed by experimental accuracy [2, 6]. In recent years, major experimental campaigns have been mounted at several laboratories to measure many different spin asymmetry combinations with proton targets. However, the electromagnetic interaction does not conserve isospin. In particular, the amplitude for the $N(\gamma,\pi)$ reaction factors into distinct isospin components, $A_{(\gamma,\pi^\pm)} = \sqrt{2}\{A_{p/n}^{I=1/2} \mp 1/3\, A^{I=3/2}\}$. Thus, while the excitation of I=3/2 Δ^* states can be entirely determined from proton target data, measurements with both neutron and proton targets are required to deduce the isospin I=1/2 amplitudes, and separate γpN^* and γnN^* couplings. Generally, the latter are poorly determined, due to the paucity of neutron reaction data.

The E06-101 experiment at Jefferson Lab, the *g14* run with the CEBAF Large Acceptance Spectrometer (CLAS) in Hall B [8], has focused on constraining photoproduction amplitudes with new spin observables from polarized neutrons. Here we report the first beam-target double polarization measurements through the resonance region of $E = \frac{1}{P_\gamma P_T}\frac{\sigma_A - \sigma_P}{\sigma_A + \sigma_P}$ in the quasi-free reaction $\gamma\, n(p) \to \pi^- p(p)$, as measured with beam (P_γ) and tar-

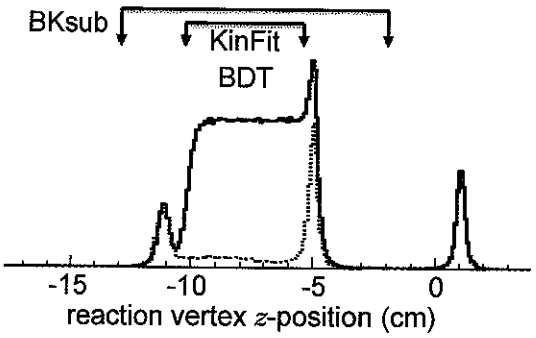

FIG. 1. Reaction vertex distance along the beam direction (z), reconstructed by tracking π^- and p in CLAS, shown for equivalent-flux data from full (*solid blue*) and empty (*dotted red*) targets. Beam entrance and exit windows generate peaks at -11 and -5 cm, respectively. A target-independent foil in the cryostat generates the peak at +1 cm. The regions included in the *BKsub* and in the *KinFit and BDT* analyses are indicated.

get polarizations (P_T) anti-parallel (A) and parallel (P) to the beam momentum, using the sign convention of [7].

Tagged photons, with circular polarization up to 85%, were generated by the bremsstrahlung of longitudinally polarized electrons, and spanned the energy range from 0.7 to 2.4 GeV. The electron polarization was periodically monitored by Møller scattering and the helicity transferred to the photon was calculated from [12]. The beam polarization was flipped in a semi-random pattern at 960 Hz by flipping the electron helicity, with a charge asymmetry between the two states of less than 10^{-3}. Photons beams were incident on 5 cm frozen-spin targets of longitudinally polarized hydrogen-deuteride (HD) in the solid phase [9–11]. D polarizations were monitored frequently in-beam with NMR [10] and averaged 26%, with relaxation times in excess of a year. A sample reconstruction of the $\pi^- p$ reaction vertex is shown in figure 1 as the solid (blue) histogram. Background reactions from the unpolarizable material of the target cell, pCTFE[C_2ClF_3] walls and Al cooling wires [9], were small. These could be directly measured by warming the cell and pumping out the HD gas (dotted red histogram). After subtraction, the deuterium of the HD provided the only source of neutrons. In the analysis of E06-101, advanced techniques such as *Kinematic Fitting* and *Boosted Decision Trees*, have been employed to study other channels with multi-particle final states and/or low cross sections. To validate the implementation of these complex methods, each has been applied to this same high-statistics channel having only charged particles in the final state, $\gamma D \to \pi^- p(p)$. These have been compared to a conventional analysis of sequential one-dimensional requirements with empty-target subtraction. Each analysis selected events with exactly one π^- and one p, both identified by the correlations between their velocities and momenta in the CLAS.

In the conventional *Background-Subtraction* (BKsub) analysis, a sequence of cuts was applied to isolate the final state. Since in the quasi-free limit the desired reaction from the neutron is 2-body, only events with an azimuthal angle difference between the p and the π^- of $180^o \pm 20^o$ degrees were accepted. The undetected *spectator* proton of the reaction $\gamma + D \to \pi^- + p + (p_s)$ was reconstructed and the square of its missing mass was required to be less than 1.1 GeV^2. Backgrounds from the target cell, including the beam-entrance and exit windows (as indicated in figure 1), were subtracted for each kinematic bin using flux-normalized empty-cell data.

Kinematic fitting (KinFit) used the constraints of energy and momentum conservation to improve the accuracy of measured quantities, and so obtained improved estimates on the momenta of undetected particles [13]. This allowed a separation of reactions with additional particles in the final state, as well as reactions on bound nucleons in the target cell material, since these deviated from elementary kinematics. This procedure also significantly suppressed high-momentum neutrons in the deuteron. In this analysis, a pre-selection based on vertex reconstruction was used to eliminated the target cell windows (as in figure 1). For each event, a confidence level, calculated for the reaction $\gamma + n \to \pi^- + p$ where the target was assumed to have the neutron mass but unknown momentum [14], was required to be ≥ 0.05.

When processing exclusive events, many kinematic variables can be constructed. Conventional *BKsub-style* analyses view each variable in different projections to 1 or 2 dimensions where *sequential* requirements are placed on the data. In contrast, multivariate *Boosted Decision Trees* (BDT) can be used to view each event in a higher dimension where all requirements can be placed *simultaneously* [15, 16]. The process creates a *forest* of logical *if-else* tests for all kinematic variables and the resulting decision trees are applied to all the information. In this application, $\pi^- + p$ candidate events are pre-selected and their reconstructed origin is required to lie within a region excluding the target cell windows (figure 1). The BDT algorithm is *trained* on the results of a Monte Carlo of the CLAS response to the reaction of interest and on the empty-cell data, and then is used to separate each event into either *signal* or *background* [17]. On average, this procedure retains about 25% more events, which results in smaller statistical uncertainties.

The final requirement common to all 3 analyses is the selection of events for which the neutron in deuterium is as close to *free* as possible, and the key experimental parameter is the momentum of the undetected (*spectator*) proton. Since different polarization observables may exhibit different sensitivities, we have chosen to determine the optimum threshold from the data itself. Studies with individual kinematic bins have shown a dilution of the E asymmetry when the $|P_{miss}|$ threshold is increased above 0.1 GeV/c, but no statistically significant change for smaller values. When averaged over the full kinematic

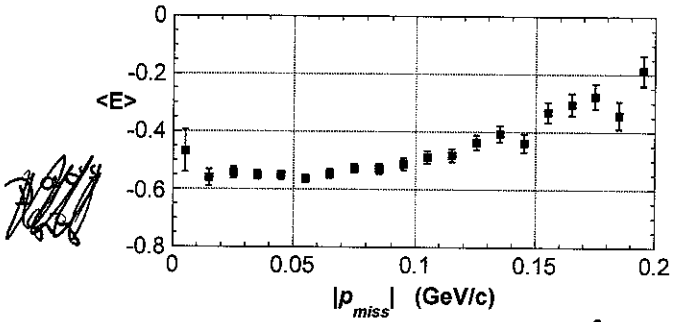

FIG. 2. E asymmetries averaged over the full ~~data set~~, as determined in the BDT analysis for $\gamma + D \to \pi^- + p + (p_{miss})$.

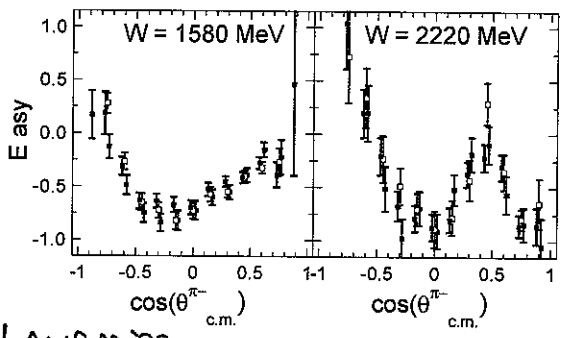

FIG. 3. Angular distributions of E asymmetries in the $\gamma n \to \pi^- p$ center of mass (cm) for two different ± 20 MeV mass bins, as determined from *BKsub* (black open circles), *KinFit* (red squares) and *BDT* (green squares) analyses, respectively. *KinFit* and *BDT* points are shifted slightly in angle for clarity.

range, the mean value of the E asymmetry, is plotted in ~~figure~~ 2 as a function of missing momentum. This average is again stable below 0.1 GeV/c but rises significantly at higher $|P_{miss}|$. Consequently, $|P_{miss}| \leq 0.1$ has been required in all 3 analyses. (There is still a slight curvature below 0.1 in ~~figure~~ 2, and extrapolations to $|P_{miss}| = 0$ would suggest a further 2% correction. However, since this could have an angle dependence [18], we have instead ~~incorporated~~ this difference into the systematic errors.)

The effect of the deuteron's D-state has been studied within an impulse calculation, including all relativistic transformations of the spin of the moving neutron [18]. Dilution of the E asymmetry can be significant whenever high spectator momenta are present, but are suppressed to negligible levels by the $|P_{miss}| \leq 0.1$ requirement.

The combination of Monte Carlo simulations of the CLAS response to quasi-free $\gamma D \to \pi^- p(p)$, including Fermi motion, together with flux-scaled empty-cell data, reproduces the observed the $|P_{miss}|$ distribution below 0.1 GeV/c, although deviations arise at higher momenta. Theoretically, the explicit effects of final state NN interactions (FSI) and πN rescattering on the E asymmetry have been investigated for the lower end of the g14 energy range [19, 20], and found to be negligible for the $\pi^- pp$ final state (but noticeable for $\pi^0 np$). From the above considerations, we regard the E asymmetries reported here as ~~the best~~ estimates for a *free* neutron target.

Asymmetries extracted from the BKsub, KinFit and BDT analyses are shown in ~~figure~~ 3 for two sample mass bins, near the low and high ends of the W range. Results from the 3 data reduction methods are statistically consistent over the full energy range. A weighted average of the results from the three analyses has been used as the best estimate of the $\pi^- p$ E asymmetries. In calculating the net uncertainty, we have used standard methods to evaluate the correlations between the analyses [21], ~~which are not complete since the different procedures result in a selection of different sets of events.~~ The resulting asymmetries, grouped in ± 20 MeV bins, are shown in ~~figure~~ 4.

Systematic uncertainties associated with event processing enter the three analyses in different ways, but total about 4% in each case. We assign an additional error of 2% to the uncorrected extrapolation to $|\vec{p}_{miss}| = 0$. A polarization uncertainty of 7% (6.0% target and 3.4% beam) represents a scale error on the data set as a whole. The total systematic uncertainty is 8%.

New Partial Wave Analyses (PWA) of π photoproduction have been carried out, augmenting the neutron data base with these new E asymmetry results. PWA from the George Washington University Data-Analysis group (SAID) [22] are shown as red bands in ~~figure~~ 4, where the band width indicates the variation across the mass bin. New PWA from the Bonn-Gatchina (BnGa) group [23] are shown as solid black curves.

The new $\pi^- p$ E asymmetries have had a significant impact on multipole solutions. To illustrate their effect, we have plotted in ~~figure~~ 4 the predictions from previous PWA solutions in a sample of three panels at low (1580 MeV), mid (1900 MeV) and high (2220 MeV) energies. Predictions from the most recent on-line versions, SAID[CM12] [24] and BnGa[2014-02] [25] are shown as the red-dotted and grey dash-dotted curves, respectively. Predictions from more recent PWA which include all currently published data [26] (but exclude our $\pi^- p$ E asymmetries) are shown as the red-dashed and black-dotted curves. While the earlier PWA solutions are close to the E data at low energies, they become wildly disparate above masses of about 1800 MeV.

As expected, the $I = 3/2$ partial waves, which are determined by proton target data, have remained essentially unaltered, while various $I = 1/2$ waves have changed substantially. As examples, in ~~figure~~ 5 we show Argand plots of the $(L^{\pi N})_{IJ}(n/p)E/M = P_{13}nM$ (top row) and $G_{17}nM$ (bottom row) partial waves. Both reveal the expected counter-clockwise phase motion near the $N(1720)3/2^+$ and $N(2190)7/2^-$ four-star resonances, whose centroids are indicated by open-black arrows [5]. Recent PWA from SAID and BnGa are plotted in the left and right columns, respectively.

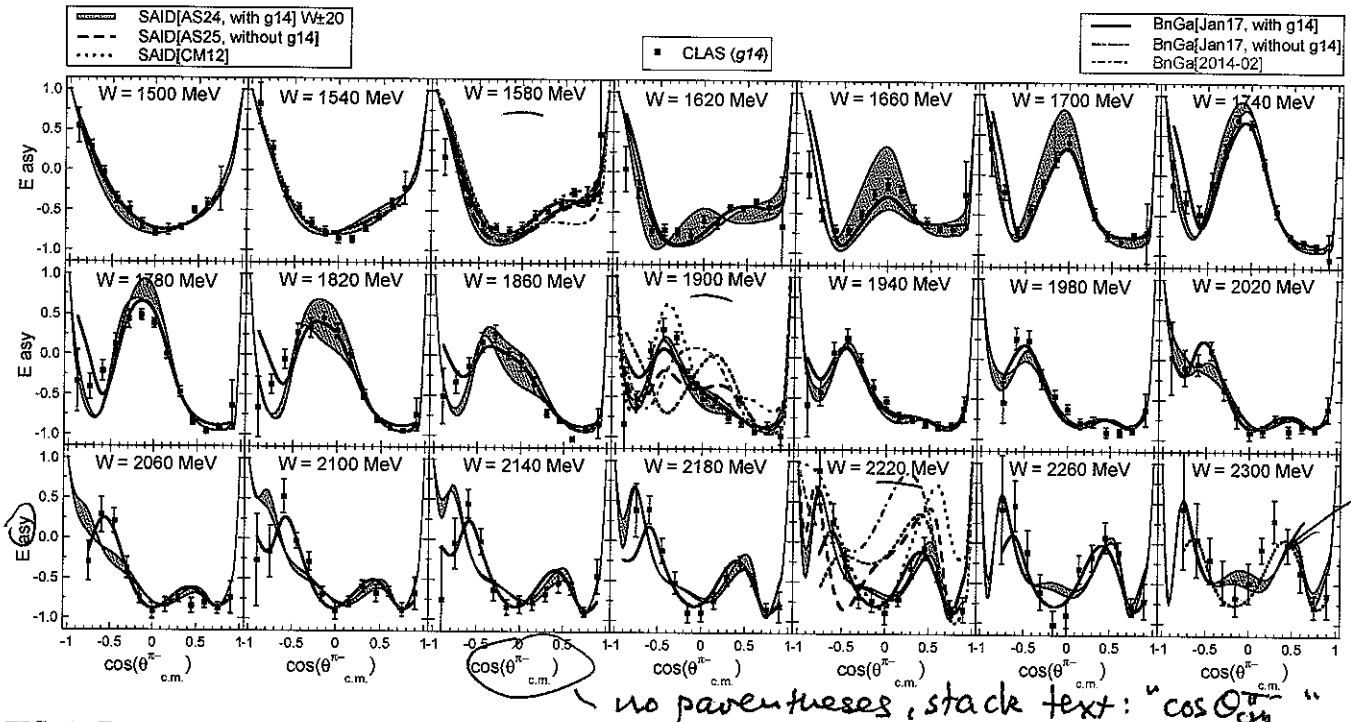

FIG. 4. E asymmetries for $\vec{\gamma}\vec{n} \to \pi^- p$ (blue squares), grouped in ±20 MeV mass bins, shown with recent PWA fits that have included these data: solid red curves from SAID [22], with shaded bands indicating variations across the energy bin; solid black lines from BnGa [23]. Also plotted at three energies (1580, 1900, 2220) are previous PWA solutions that did not include the present data set in the multipole search: red-dotted curves from SAID[CM12], based on all data up to 2012 [24]; red-dashed curves from a SAID[AS25] solution including all currently published data; grey dot-dashed curves from BnGa[2014-02], based on all data up to 2014 [25]; black short-dashed curves show a BnGa PWA using all available published data.

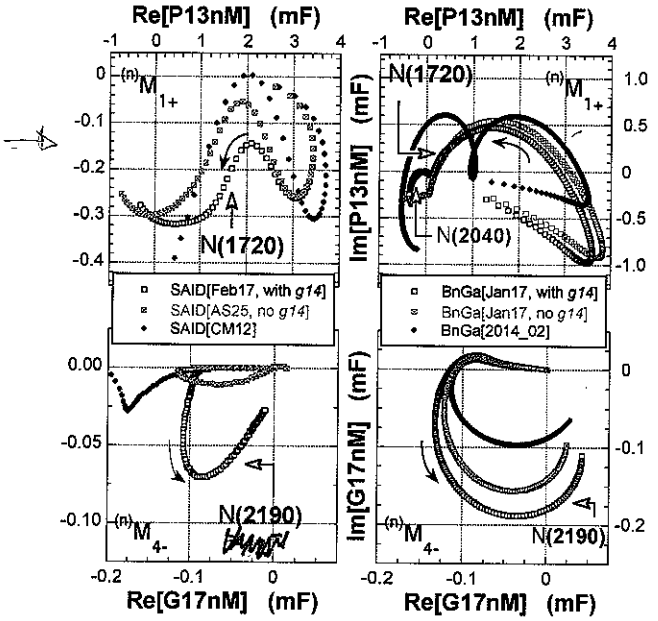

FIG. 5. Argand plots of the $P_{13}nM$ (top) and $G_{17}nM$ (bottom) multipoles from π-threshold to W=2300 MeV. Solid arrows indicate increasing W. SAID and BnGa PWA are shown in the left and right columns, respectively. As in the legend, red diamonds are the on-line versions [24, 25], light-green squares include all previously published data, and dark-green circles include all data including the new E asymmetries.

The γnN^* couplings are parameterized by the transverse helicity amplitudes. For the $N(2190)7/2^-$, the new G_{17} BnGa multipoles (dark green squares) result in $\pm|A_n^{1/2}| = +30 \pm 7$ and $\pm|A_n^{3/2}| = -23 \pm 8$, in units of $10^{-3}\text{GeV}^{-1/2}$. This is significantly different from previous BnGa values of -15 ± 12 and -33 ± 20 [5, 27], respectively. The corresponding new SAID PWA results in $\pm|A_n^{1/2}| = +6 \pm 1$ and $\pm|A_n^{3/2}| = -21 \pm 4$. (The G_{17} wave in previous SAID analyses had been too small to extract couplings.) With the inclusion of the new E asymmetry data, the extracted $\pm|A_n^{3/2}|$ amplitudes are in agreement and the $\pm|A_n^{1/2}|$ values now have the same sign.

From changes in the P_{13} wave (top row of figure 5), the SAID PWA has extracted new values of $\pm|A_n^{1/2}| = -19 \pm 4$ and $\pm|A_n^{3/2}| = -3 \pm 1$ for the $N(1720)3/2^+$. While changes are also evident in the BnGa PWA, the proximity of the ρ-threshold complicates this coupled-channel analysis, and revised couplings will be presented elsewhere. The new BnGa PWA also shows resonance-like phase motion near the mass of a one-star $N(2040)3/2^+$ (grey arrow in figure 5). This state had not been explicitly included in their PWA and is now under study.

Several other $I = 1/2$ waves have also changed significantly. The influence of other data sets on these are currently under study, (since both charge channels are

for the first time

required to construct the isospin amplitude, $A_n^{I=1/2} = [\sqrt{2}A_{\pi^-p} - A_{\pi^0 n}]/3$, and FSI are more problematic for the $\pi^0 nn$ final state).

In summary, the beam-target helicity asymmetry has been measured for the $\vec{\gamma}\vec{D} \to \pi^- p(p)$ reaction, and analysis constraints have been used to deduce the E polarization asymmetry for a neutron target across the resonance region. Their inclusion in new PWA calculations have improved the determination of γnN^* couplings.

We are grateful for the assistance of the JLab Hall B and Accelerator technical staff. This work was supported by the US Department of Energy, Office of Nuclear Physics Division, under contract DE-AC05-06OR23177 under which Jefferson Science Associates operate Jefferson Laboratory, by the US National Science Foundation, and by the Italian Istituto Nazionale di Fisica Nucleare.

---

* corresponding authors: sandorfi@JLab.org
fklein@JLab.org

[1] A.M. Sandorfi, J. Phys. Conf. **424**, 012001 (2013).
[2] A.M. Sandorfi, S. Hoblit, H. Kamano and T-S. H. Lee, J. Phys. G**38**, 053001 (2011).
[3] S. Capstick and W. Roberts, Phys. Rev. D**58** 074011 (1998).
[4] R.G. Edwards, *et al.*, Phys. Rev. D**84** 074508 (2011).
[5] C. Patrignani, *et al.*, Chin. Phys. C**40** 100001 (2016).
[6] S. Hoblit, *et al.*, AIP Conf. Proc. **1432**, 231 (2012).
[7] A.M. Sandorfi, B. Dey, A.V. Sarantsev, L. Tiator and R.L. Workman, AIP Conf. Proc. **1432**, 219 (2012); arXiv:1108.5411v2.
[8] B. Mecking, *et al.*, Nucl. Inst. Meth. Phys. Res. A**503**, 513 (2003).
[9] C.D. Bass, *et al.*, Nucl. Inst. Meth. Phys. Res. A**737**, 107 (2014).
[10] M.M. Lowry, *et al.*, Nucl. Inst. Meth. Phys. Res. A**815**, 31 (2016).
[11] X. Wei, *et al.*, Proc. of Science PoS (PSTP 2013) 16.
[12] H. Olsen and L.C. Maximon, Phys. Rev. **114**, 887 (1959).
[13] A.G. Frodesen and O. Skjeggestad, *Probability and Statistics in Particle Physics*, Universitetsforlaget, Bergen, Norway; ISBN 82-00-01906-3, 1979.
[14] P. Peng, Ph.D. thesis, University of Virginia (2015); http://search.lib.virginia.edu/catalog/libra-oa:10965.
[15] H. Drucker and C. Cortes, Adv. Neural Inform. Process Sys. **8** (1996).
[16] A. Hoecker, *et al.*, arXiv:physics/0703039.
[17] D. Ho, Ph.D. thesis, Carnegie Mellon University (2015); http://repository.cmu.edu/dissertations/590.
[18] T.-S. H. Lee (*priv. comm.*)
[19] A. Fix and H. Arenhoevel, Phys. Rev. C**72**, 064005 (2005).
[20] J. Wu, T. Sato and T-S. H. Lee, Phys. Rev. C**91**, 035203 (2015).
[21] M. Schmelling, Physica Scripta **51**, 676 (1995).
[22] R.L. Workman, *et al.*, http://gwdac.phys.gwu.edu.
[23] V.A. Nikonov, *et al.*, http://pwa.hiskp.uni-bonn.de.
[24] R.L. Workman, *et al.*, Phys. Rev. C**86**, 015202 (2012).
[25] E. Gutz, *et al.*, Eur. Phys. J. A**50**, 74 (2014).
[26] P. Adlarson, *et al.*, Phys. Rev. C**92**, 024617 (2015); and references therein.
[27] A.V. Anisovich, *et al.*, Eur. Phys. J. A**49**, 67 (2013).

[8] . . .

Fix order.

Need to give better references to these models.

This draft is in quite good shape. We need to move on this to submit it before Mainz scoops us. If they publish first we can't get into Phys. Rev. Lett!

The length seems fine. Could add a paragraph or two.